

TARC: Time-Adaptive Robotic Control

Arnav Sukhija¹, Lenart Treven¹, Jin Cheng¹, Florian Dörfler², Stelian Coros¹, Andreas Krause¹

Abstract—Fixed-frequency control in robotics imposes a trade-off between the efficiency of low-frequency control and the robustness of high-frequency control, a limitation not seen in adaptable biological systems. We address this with a reinforcement learning approach in which policies jointly select control actions and their application durations, enabling robots to autonomously modulate their control frequency in response to situational demands. We validate our method with zero-shot sim-to-real experiments on two distinct hardware platforms: a high-speed RC car and a quadrupedal robot. Our method matches or outperforms fixed-frequency baselines in terms of rewards while significantly reducing the control frequency and exhibiting adaptive frequency control under real-world conditions.

I. INTRODUCTION

Efficient and adaptive control is a hallmark of intelligent systems. Biological systems, for instance, masterfully adapt their control effort to the complexity of a situation [1], [2]. Walking on a sidewalk requires little conscious control, our steps are automatic, and corrections are infrequent. In contrast, walking on a slack line requires constant attention, frequent corrections, and adjustments to maintain balance. This ability to dynamically modulate control frequency is fundamental to the robustness and efficiency of human motor skills [1].

In sharp contrast, most existing control methods in robotics rely on a fixed control frequency in all scenarios [3]–[7]. For example, a self-driving car is controlled at the same frequency when driving straight compared to when performing a complicated drift maneuver. Although adaptability has been extensively studied in human-robot interaction and collaborative contexts [8]–[10], this dynamic modulation of control frequency remains under-addressed.

The fixed-frequency approach, in turn, forces a fundamental compromise. A too low control frequency, while computationally cheap, risks failure when the controller must react to sudden changes in its state or environment. Conversely, a too high frequency ensures robustness and reactivity but comes at a significant and often unnecessary computational cost. In robotics, this trade-off leads to a preference for the latter approach, accepting a high computational burden to guarantee performance in the worst-case scenario [3]–[7].

¹The authors are with the Department of Computer Science, ETH Zurich, Zurich Switzerland. {asukhija, trevenl, jicheng, scoros, krausea}@ethz.ch

²Florian Dörfler is with the Department of Information Technology and Electrical Engineering, ETH Zurich, Zurich, Switzerland. dorfler@ethz.ch

Project website: <https://arnavsukhija.github.io/projects/tarc/>. Supplementary video: <https://youtu.be/w0y6uunPYc>

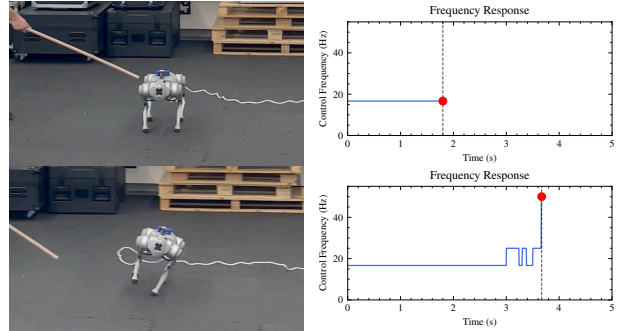


Fig. 1: The performance of TARC on scenarios requiring adaptation in control frequency. The *quadruped's* control frequency spikes when experiencing a push, demonstrating state-dependent frequency modulation.

In this work, we present **Time-Adaptive Robotic Control (TARC)**, a reinforcement learning (RL) approach that enables robots to modulate their control frequency. Our policies learn to jointly output a control action and its application duration, building on the TaCoS framework [11], which allows this joint output to be learned using any standard RL algorithm. We demonstrate the effectiveness and generalizability of TARC via zero-shot sim-to-real deployment on two distinct dynamic platforms. Its core capability of modulating control frequency in response to situational demands is illustrated in Fig. 1. Our key contributions are summarized as follows:

- We introduce an adaptive frequency control method and validate it on two dynamically distinct robotic tasks: a high-speed RC car drifting and the quadruped locomotion.
- We demonstrate that such adaptive policies achieve task performance comparable to fixed-frequency baselines while requiring less control interventions.
- We show that our learned policies autonomously modulate their control frequency in response to situational demands.

II. RELATED WORK

A. Choice of Control Frequency in Robotic Systems

Traditional robotic control schemes often operate at a fixed frequency, which introduces several practical limitations. Fixed-frequency controllers can be wasteful if the frequency is too high, and their limitations have been extensively addressed in recent literature. Park et al. [12] and Amin et al. [13] show that variable action durations can significantly improve learning performance. Although high frequencies can

ensure reactivity, they incur significant computational costs and can hinder training [14], [15]. In contrast, low-frequency control is efficient and can improve latency insensitivity [16], but it risks instability when rapid reactions are needed. These challenges are not unique to learning-based methods; Nguyen et al. [17] challenge the "one frequency for all" intuition by using different control frequencies for different scenarios. They consider a dynamic jumping maneuver on legged robots using Model Predictive Control (MPC) and observe more robust results with different control frequencies for the in-flight phase and the ground phase. Similarly, Li et al. [18] use a two-agent framework for humanoid locomotion, where a high-frequency agent stabilizes the upper body while a lower-frequency agent controls the gait, highlighting the benefit of specialized frequencies for tasks with mismatched dynamics. These previous works highlight the trade-offs of frequency selection and motivate the need for more flexible, adaptive control strategies.

B. Adaptive Frequency Control

To overcome these limitations, recent research has explored methods that adapt the control frequency during run-time. A significant amount of research has been conducted on repetitive action reinforcement learning, which enables agents to repeat actions over multiple time steps [19]–[22]. Furthermore, Wang et al. [15], [23] explore variable time-step reinforcement learning with adaptive control frequencies where the agent adapts the control frequencies based on task requirements. Their method extends Soft-Actor-Critic (SAC) [24] with variable time steps and reward shaping, enabling the agent to select both which action to take and its execution duration using additional hyperparameter tuning. Similar concepts have appeared in MPC, where neural-augmented methods simultaneously optimize step location, step duration, and contact forces for natural variable-frequency locomotion [25].

Another related direction is event- and self-triggered control [26], [27], in which control updates are executed only when predefined stability conditions are violated. These methods ensure efficiency by minimizing unnecessary interventions, but they typically rely on hand-crafted triggering conditions and remain limited to reactive, safety-driven updates.

In contrast, our work generalizes these concepts. We use the flexible TaCoS framework [11], which formalizes an extended Markov Decision Process (MDP) that any standard RL algorithm can solve without extensive reward shaping or hyperparameter adjustment.

III. METHOD

In this section, we describe our methodology for learning time-adaptive control policies that jointly predict the next action and their application durations. Fig. 2 provides an overview of our methodology.

A. Time-Adaptive Control

To obtain time-adaptive control policies, we adopt the interaction cost setting of the *Time-adaptive Control and*

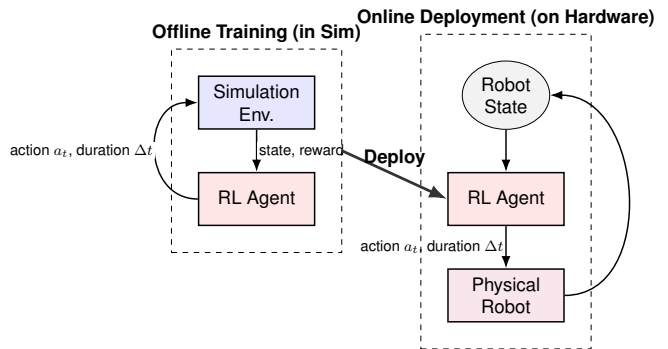


Fig. 2: Overview of our framework. The RL agent outputs an action a_t and an application duration Δt , which allows the policy to modulate control frequency. We train completely offline in simulation (left), and deploy the policy zero-shot on the hardware (right).

Sensing (TaCoS) framework [11]. TaCoS transforms a continuous-time MDP to an extended discrete-time MDP which any standard RL algorithm can solve.

Although the intricate system dynamics behind both of our robotic platforms is continuous-time, their hardware implementations work in discrete-time, which means that control is applied at a fixed frequency f_{max} . Thus, we adapt the framework to a discrete-time setting in which the agent may choose to repeat actions over multiple control steps. This allows the policy to implicitly select the applied control frequency.

1) *Policy Class*: Let $i \in \mathbb{N}$ denote the maximum repetition count. In our setting, this corresponds to the maximum number of control steps that the agent can select as the action's application duration. The policy class we consider extends a standard action-selection policy to include time-adaptive duration selection:

Definition 1 (Time-Adaptive Policy π): Let \mathcal{X} be the state space, \mathcal{A} the action space, and $T \in \mathbb{N}$ the episode horizon. At step $t \in \{0, 1, \dots, T\}$, let the agent observe the state $s_t = (x_t, t) \in \mathcal{X} \times \{0, 1, \dots, T\}$, where $x_t \in \mathcal{X}$ is the environment state. A **time-adaptive policy** is a function $\pi : \mathcal{X} \times \{0, 1, \dots, T\} \rightarrow \mathcal{A} \times \{1, 2, \dots, i\}$ such that

$$\pi(s_t) = (a_t, \Delta t) \quad (1)$$

where $a_t \in \mathcal{A}$ is the action and $\Delta t \in \{1, 2, \dots, i\}$ the application duration.

We refer to a controller using such a policy as **TARC- i** . Since control actions are kept constant for the Δt time steps, the resulting control frequency dynamically varies as

$$f = \frac{f_{max}}{\Delta t} \in \left[\frac{f_{max}}{i}, f_{max} \right] \quad (2)$$

2) *Switch Cost and Reward*: To encourage sparser control intervention and thus lower control frequencies, we penalize the agent for each action switch with a fixed cost $c \in \mathbb{R}$ (see the interaction cost formulation in the TaCoS paper [11]). The goal is to discourage high-frequency control actions unless they are necessary for task performance.

Definition 2 (Reward function R): Let $r : \mathcal{X} \times \mathcal{A} \rightarrow \mathbb{R}$ denote the original reward function of the underlying MDP, $\gamma \in (0, 1]$ be the discount factor, $c \in \mathbb{R}$ the switch cost, $s_t = (x_t, t)$ the augmented state at time t , $u_t = (a_t, \Delta t)$ the augmented action. We define the reward function R of our discrete-time augmented MDP as:

$$R(s_t, u_t) = \left(\sum_{k=0}^{\Delta t-1} \gamma^k r(x_{t+k}, a_t) \right) - c \quad (3)$$

where

- x_{t+k} is the state observed at time $t+k$ by repeatedly executing a_t
- a_t is held constant for Δt steps

This reward structure encourages the agent to maximize task performance while minimizing unnecessary interventions through the switch penalty. This hyperparameter is tuned to align with the specific control requirements, the degree to which low control frequencies are encouraged, and the characteristics of the robotic platform.

If c is too low, the agent tends to favor high-frequency control, similar to the fixed-rate baseline. In contrast, a very high c can discourage necessary control updates, causing the agent to repeat actions excessively or act conservatively. Selecting an appropriate value of c is important to balance the costs of control intervention with responsiveness.

For each robotic platform, we provide the values of c used in our experiments in section IV.

IV. EXPERIMENTAL SETUP

For both platforms, we compare our TARC policies with a fixed-frequency baseline controller operating at the base control frequency f_{max} . The baseline simply picks an action at each step and acts within the standard, non-augmented MDP.

Training is done offline with the help of simulators and deployed zero-shot on to the real hardware platform. All policies are optimized using Proximal Policy Optimization (PPO) [28], [29]. We consider several variants of adaptive policies as per Definition 1, specifically, **TARC-3**, **TARC-4**, **TARC-5**, **TARC-10**.

For our evaluations, we consider the following performance metrics, both directly reported on the hardware in Section V:

- **Total Reward:** We report the cumulative reward per episode under two conditions. The **penalized reward** includes the switch cost c to evaluate how well the policy balances task performance against the cost of frequent control interventions. The **unpenalized reward** excludes this cost to provide a direct measure of pure task performance.
- **Average Control Frequency:** The average number of control actions applied per second (Hz). This metric directly quantifies the policy’s intervention rate.



Fig. 3: Desired reverse parking maneuver which involves rotating the car 180° and parking approx. 2m away

A. RC Car

The RC car is similar to those of Bhardwaj et al. and Sukhija et al. [30], [31]. The car’s state is six-dimensional, capturing position, orientation, and linear/angular velocities, while the input is two-dimensional (steering and throttle). The control commands are executed at a base frequency of $f_{max} = 30\text{Hz}$. For state estimation, we use the OptiTrack motion capture system [32], which ensures robust feedback.

The environment incorporates a dynamics model based on Kabzan et al. [33], using the Pacejka tire model [34] to better model drifting and tire-road interaction effects. For better sim-to-real transfer, we use domain randomization: physical parameters such as center of mass, mass, tire stiffness (drifting), and motor power are sampled across episodes [35].

Additionally, we observe that there is a significant delay (approx. 80 ms) between transmission and execution of the control signals on the car. To account for this delay, we augment the current underlying state x_t with the last three actions $[a_{t-3}, a_{t-2}, a_{t-1}]$. This creates an intermediate 12-dimensional state representation, which is then further augmented for the TARC policies as described in Definition 1.

The RL task is a reverse parking maneuver: starting approximately 2m from a target position, the car must rotate 180°, typically requiring a drift (see Fig. 3). This scenario is chosen to have high and low control demand, so that a non-adaptive f_{max} baseline can be compared against the adaptive controller. This task is considered over one episode of 200 control steps at frequency f_{max} , which corresponds to $\frac{200}{30} = 6.6$ seconds.

To that extent, we formulate the following reward function $r : \mathcal{X} \times \mathcal{A} \rightarrow \mathbb{R}$ for the RC car:

$$r(x_t, a_t) = r_{state}(x_t) - w \cdot \|a_t\| \quad (4)$$

This reward function, the hyperparameters, and the simulation environment are the same as those used by Rothfuss et al. [36]¹. The reward function is based on the tolerance reward from Tassa et al. [37]. The tolerance function r_{state} gives higher rewards when the agent is close to a desired state, that is, in the case of the RC car, the target position. The “closeness” is quantified using a margin parameter for the reward function. Rothfuss et al. [36] use a margin of 20,

¹Official implementation: https://github.com/lasgroup/simulation_transfer

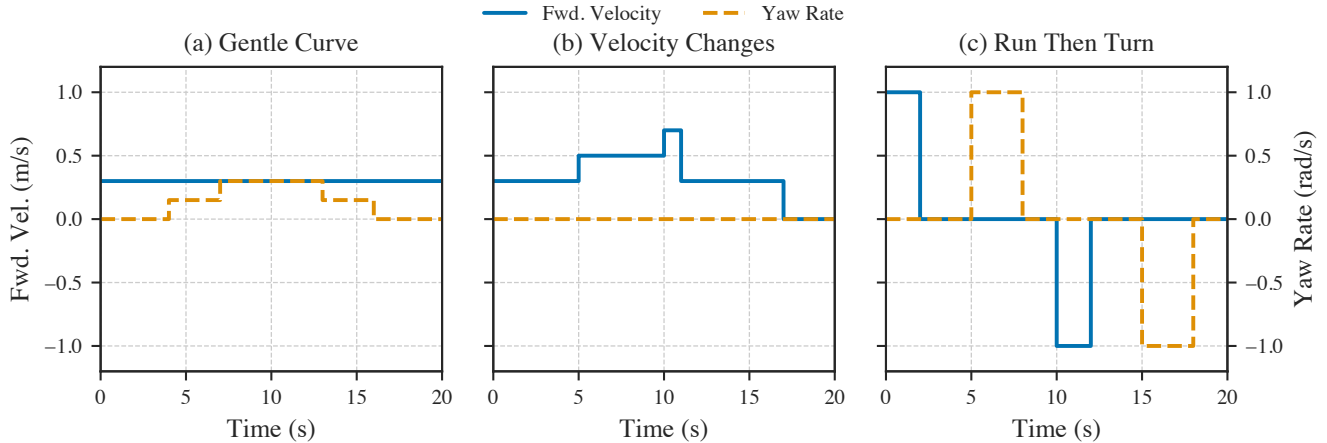


Fig. 4: The three evaluation scenarios for the Unitree Go1, defined by their command profiles over a 20-second episode. Each plot shows the commanded forward velocity (solid blue line, left axis) and yaw rate (dashed orange line, right axis) over time for each scenario (a) Gentle Curve, (b) Velocity Changes, and (c) Run Then Turn.

while also penalizing large steering angles and throttles with a weight factor w . In our experiments, we keep $w = 0.005$.

This reward function is used as a basis for the reward function R of our adaptive controllers according to Definition 2. The switch cost was empirically tuned in simulation to balance task performance (rewards) with control frequency. We observed that lower values did not sufficiently penalize action switches, while higher values hindered the agent’s reactivity. Based on these observations, we used a value of $c = 0.1$.

B. The quadruped

For the quadrupedal locomotion task, we use the Unitree Go1 [38]. The Go1 is a quadruped robot equipped with four legs, each possessing three degrees of freedom, resulting in a 12-dimensional action space and a 48-dimensional state space comprising of velocities, joint positions, and joint velocities.

To achieve efficient sim-to-real transfer, we use MuJoCo Playground [39], a simulation and deployment platform optimized for ease of transfer of RL policy from simulation to hardware. This framework enables us to execute policies identically in simulation and on physical Go1 hardware, using a unified interface that issues control signals at a base frequency of $f_{max} = 50\text{Hz}$ via the ONNX runtime [40].

1) *Joystick Locomotion Task:* For the goal of the policies, we consider the joystick locomotion tasks [41], [42], where, at each timestep, the agent receives a target command specifying the desired forward velocity, lateral velocity and yaw rate for the robot trunk. The policy’s task is to then map these high-dimensional commands accurately to actual joint targets.

Our method operates within a hierarchical control architecture, similar to prior work [4], [43]. A high-level RL policy provides desired joint targets, which are then tracked by a low-level PD controller that computes motor torques. We apply adaptive control to the high-level policy layer, whereas

the fixed-frequency baseline computes the targets at a rate of 50 Hz. The low-level PD controller is left untouched, thus, once joint targets are issued, stabilization and torque tracking are handled in the same way across both adaptive and fixed-frequency baselines.

Training is performed with the MuJoCo Playground Flat-Terrain Joystick environment, leveraging domain randomization [35] to promote robust policy transferability, and an asymmetric actor-critic setup [44] for better training performance. For further details on the underlying MDP formulation of the quadruped, individual components of the reward function, and simulation environment, we refer the reader to the MuJoCo Playground paper [39].

Thus, our methodology results in an extension of the setup from MuJoCo playground with adaptive control frequency: policies are trained with upper and lower frequency bounds, learning to dynamically select the intervention rate within these constraints based on the demands of the locomotion task. Similarly to the RC Car, we empirically tested different switch costs in simulation. We observed no control frequency decrease with switch costs lower than 0.001 and with switch costs greater than 0.01, the reward did not improve with more learning time and stayed low throughout the training process. A value of $c = 0.005$ provided the most effective trade-off.

2) *Evaluation Scenarios:* To evaluate generalization and the effectiveness of our time-adaptive policies, we deploy our policies on the hardware and test them on three distinct scenarios, each conducted over a 20-second episode. Importantly, these specific command profiles were not encountered during training as such, the agent was simply trained to map joystick commands to actual joint targets, and we test the performance of this in these three different scenarios.

- **Gentle Curve:** The robot receives time-varying joystick commands that guide it along a smooth and predictable low-speed curve.
- **Velocity Changes:** The robot is commanded to walk

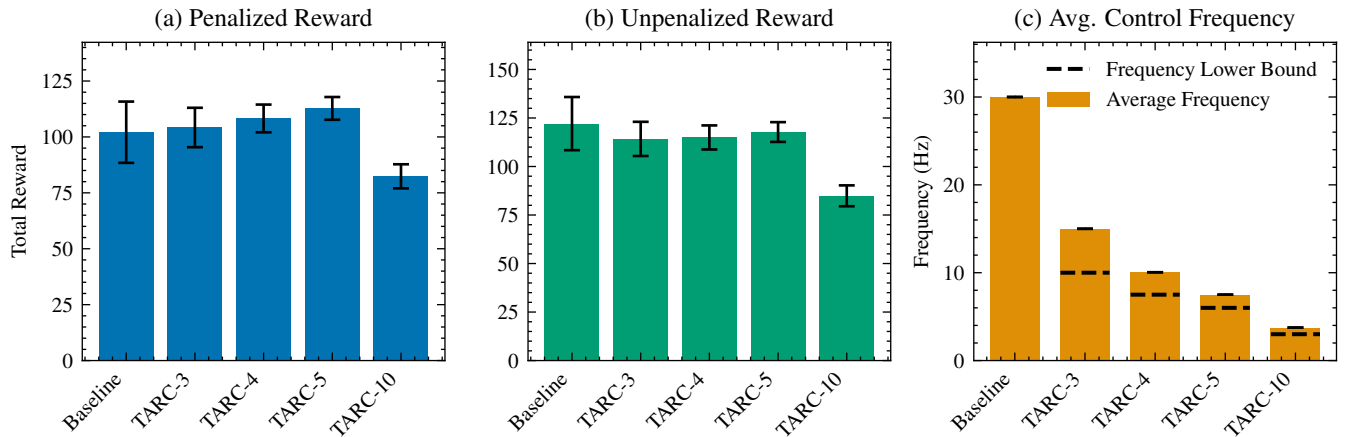


Fig. 5: Performance comparison of controllers on the RC Car task averaged over 5 seeds. The subplots show: (a) Total reward penalized with $c = 0.1$. (b) Total reward excluding the penalty (c) Average control frequency over the episode

straight at varying speeds, exposing the agent to different magnitudes of the same direction command.

- **Run Then Turn** The robot begins with a running command, followed by an abrupt switch to a in-place turn command, testing the agent’s reactivity and adaptability to sudden changes.

Representative command profiles for each scenario are shown in Fig. 4.

V. RESULTS AND DISCUSSION

In this section, we present the results of TARC applied to the RC car and Unitree Go1. For both platforms, we evaluate policy performance on total reward (with and without switch cost penalties) and average control frequency, reporting the mean and standard error over 5 random seeds.

A. RC Car

We first analyze the hardware performance of the RC car using the reward formulation defined in (4) and the formulation of Definition 2. Our results are summarized in Fig. 5. The TARC policies achieve a higher penalized reward than the baseline (Fig. 5a), a direct result of their lower control frequencies (Fig. 5c) which incur fewer switching penalties. In the unpenalized setting (Fig. 5b), while the mean rewards are comparable, the TARC policies exhibit significantly smaller variance, indicating more robust and consistent hardware performance.

The notable exception is TARC-10, which shows a clear degradation in hardware reward. This result is counterintuitive; According to our formulation in Definition 1 and (2), a higher maximum repetition count i provides the policy with the greatest flexibility by giving it access to a larger range of control frequencies. With this flexibility, the TARC-10 agent could have chosen to operate at a higher frequency if it were optimal. However, the simulation and hardware comparison in Fig. 6 reveals why this did not translate to better real-world performance. Although all TARC policies perform strongly in simulation (Fig. 6(a,b)), the figure vividly illustrates the amplified sim-to-real gap for TARC-10. This confirms that its

longer open-loop control intervals (up to 10 steps) are more sensitive to inaccuracies in the approximated dynamics.

Finally, Fig. 5c shows that TARC policies operate at less than half the frequency of the baseline. Furthermore, Fig. 6c reveals that the policy’s learned control frequency strategy transfers almost perfectly. The average frequencies selected by TARC agents are nearly identical between simulation and hardware, with negligible variance. For this task, the agents in both domains converge to a consistent, low-frequency strategy as the optimal solution. However, unlike fixed action repetition methods, our approach allows the policy to discover the optimal rate autonomously, illustrating the benefit of learning state-dependent control durations.

In addition to frequency and reward, we evaluated the smoothness of the motor commands on hardware by measuring the jitter $\|a_t - a_{t-1}\|$, that is, the change in motor input between two consecutive steps over time. We report the mean and standard error of this data across 3 seeds on the TARC-4 policies. As shown in Fig. 7, TARC policies produce smaller changes in motor command compared to the high-frequency baseline. This reduction in throttle delta demonstrates that high-frequency controllers lead to unnecessarily rapid actuation changes, which can cause increased mechanical wear, energy inefficiency, and control noise in hardware systems. By learning to minimize the intervention rate, TARC not only reduces computational and switching penalties, but also delivers smoother, more hardware-friendly actuation patterns.

B. The Unitree Go1

We evaluate our time-adaptive control approach on the Unitree Go1 across the three scenarios represented in Fig. 4: Gentle Curve, Velocity Changes, and Run Then Turn. Using the reward function from MuJoCo Playground [39] and the reward formulation according to Definition 2, we assess performance in both penalized and unpenalized settings and measure the average control frequency per episode. The results are summarized in Fig. 8.

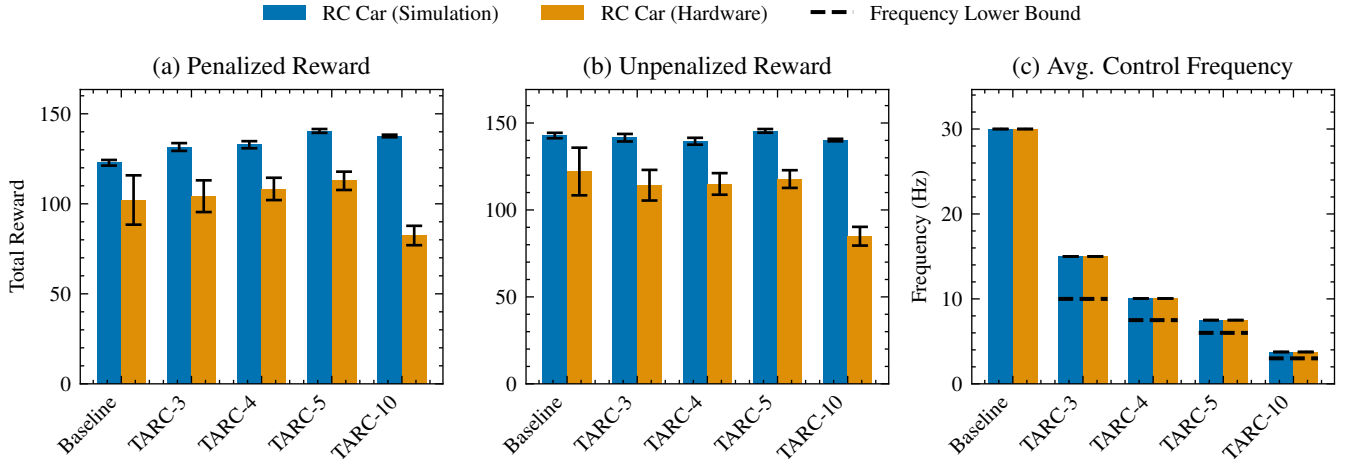


Fig. 6: Comparison of Simulation and Hardware performance for the TARC policies on the RC car. (a, b) A sim-to-real gap in reward is visible for all controllers and is most pronounced for TARC-10, highlighting the effect of longer open-loop execution. (c) In contrast, the learned average control frequency transfers almost perfectly from simulation to hardware, demonstrating the robustness of the learned efficiency strategy.

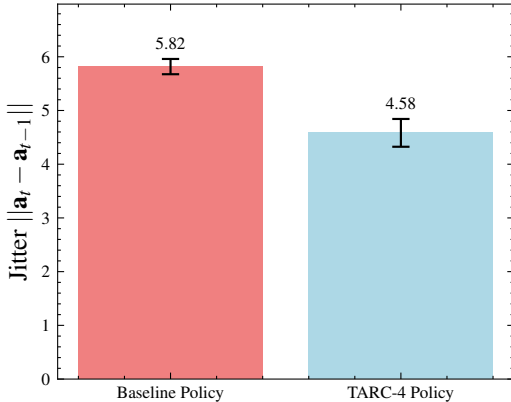


Fig. 7: Jitter of the throttle data across time for TARC policies and the fixed-frequency baseline. TARC produces smoother motor commands with lower deltas, showing that reducing high-frequency interventions avoids unnecessary command oscillations.

Fig. 8a shows that adaptive controllers achieve higher penalized rewards than the baseline in all scenarios. The differences between the TARC policies are smaller than those observed on the RC car, likely due to the lower switch cost $c = 0.005$ employed and the superior sim-to-real transfer to the Go1 using the powerful MuJoCo Playground simulator. Among the adaptive controllers, TARC-4 consistently attains the best performance with the highest penalized reward and the smallest standard error. The baseline performs particularly poorly in the more challenging Run Then Turn scenario, underscoring the robustness benefits of frequency adaptation. Additionally, TARC-4, TARC-5, and TARC-10 exhibit reduced variance compared to the baseline, highlighting their more consistent performance. In the unpenalized setting (Fig. 8b), the rewards are broadly

comparable, although TARC-10’s performance is slightly lower. This again suggests limitations of open-loop action repetition under greater durations with sim-to-real transfer, the impact although, remains marginal due to the accurate simulation environment. Furthermore, since the reward function is optimized to get smoother actions, similarly to the TARC policies, the baseline tends not to vary torques significantly over time.

The frequency analysis in Fig. 8c indicates that the average control frequency can be reduced by at least half relative to the baseline, reflecting what we observe in the RC car. Frequencies are lower on the simpler Gentle Curve scenario and increase for Velocity Changes and Run Then Turn, reflecting adaptive modulation in response to state difficulty. Furthermore, despite greater frequency flexibility, the differences in control frequency between TARC-4, TARC-5, and TARC-10 remain modest, demonstrating the agent’s capacity to select higher frequencies when necessary.

To further demonstrate adaptability and robustness, we subject the controllers to perturbations and analyze their control frequency responses. Fig. 9 vividly illustrates the resulting adaptive behavior. The policy maintains a low and efficient control rate of 16.7Hz during standstill (Fig. 9a). When pushed, it instantaneously increases its frequency to the maximum 50Hz to handle the more complex critical state in the air and ensure a stable recovery (Fig. 9b). As soon as a stable state is restored, the frequency immediately returns to the low rate (Fig. 9c). In contrast, a fixed-frequency baseline would have used 50Hz throughout the entire scenario, incurring unnecessary costs during periods of stability.

VI. CONCLUSION

In this work, we presented Time-Adaptive Robotic Control (TARC), an adaptive frequency control approach. TARC enables reinforcement learning policies to jointly optimize both

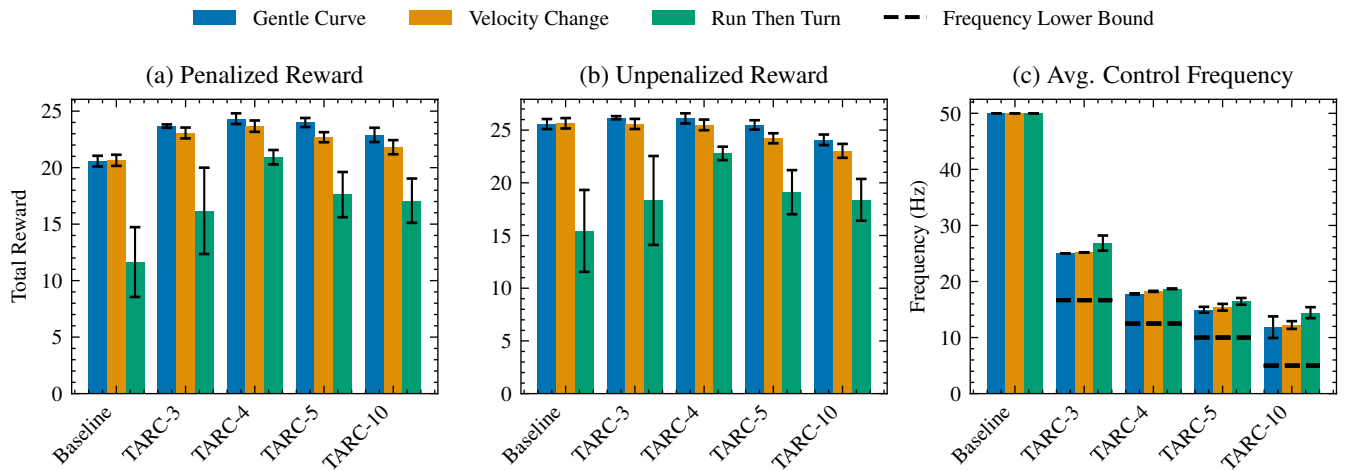


Fig. 8: Performance and efficiency metrics for the Unitree Go1 across the three evaluation scenarios. The subplots show a comparison of the baseline controller against the TARC variants on: (a) total reward with a switch cost of 0.005, (b) total reward without the penalty, and (c) the resulting average control frequency.

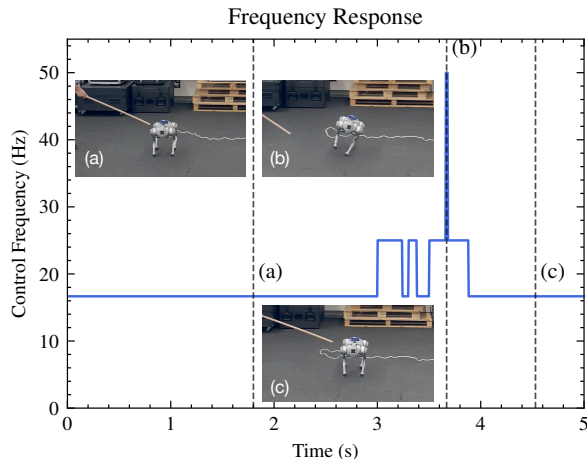


Fig. 9: The frequency response of **TARC-4** to an external perturbation on the Go1. We observe the controller uses a low frequency (16.7Hz) in a stable standstill (a, c) but immediately increases its frequency to the maximum (50Hz) to counteract the push while airborne (b). This dynamic modulation is a key benefit of adaptive frequency control.

control actions and their application durations. This allows the agent to dynamically modulate its control frequency, naturally balancing performance and efficiency without requiring specialized reward shaping.

We validated our approach via zero-shot sim-to-real deployment on two distinct robotic platforms, a drifting RC car and a quadruped. Across these platforms, our method matched or outperformed the baselines in terms of rewards while significantly reducing the control frequency. Furthermore, we exposed the Go1 to perturbations that revealed a state-dependent adaptation in control frequency, similar to how humans increase effort in challenging situations.

A key limitation of our current approach is the reliance on a fixed, empirically-tuned switch cost, which requires manual selection for new platforms. A promising direction for future work is to explore state-action-dependent switch cost functions $c(x_t, a_t)$, which would allow the policy to learn a nuanced trade-off between making cheap exploratory changes in safe states and heavily penalizing large and destabilizing actions in critical ones.

VII. ACKNOWLEDGEMENTS

This project has received funding from the Swiss National Science Foundation under NCCR Automation, grant agreement 51NF40 180545.

REFERENCES

- [1] F. Crevecoeur, J. L. Thonnard, and P. Lefèvre, “A very fast time scale of human motor adaptation: Within movement adjustments of internal representations during reaching,” *eNeuro*, vol. 7, no. 1, pp. ENEURO.0149–19.2019, 2020. [Online]. Available: <https://doi.org/10.1523/ENEURO.0149-19.2019>
- [2] J. Babič, E. Oztop, and M. Kawato, “Human motor adaptation in whole body motion,” *Scientific Reports*, vol. 6, no. 1, p. 32868, 2016. [Online]. Available: <https://doi.org/10.1038/srep32868>
- [3] J. Hwangbo, J. Lee, A. Dosovitskiy, D. Bellicoso, V. Tsounis, V. Koltun, and M. Hutter, “Learning agile and dynamic motor skills for legged robots,” *Science Robotics*, vol. 4, no. 26, 2019. [Online]. Available: <http://dx.doi.org/10.1126/scirobotics.aau5872>
- [4] J. Di Carlo, P. M. Wensing, B. Katz, G. Bledt, and S. Kim, “Dynamic locomotion in the mit cheetah 3 through convex model-predictive control,” in *2018 IEEE/RSJ International Conference on Intelligent Robots and Systems (IROS)*, 2018, pp. 1–9.
- [5] Y. Wu, W. Niu, L. Kong, X. Yu, and W. He, “Fixed-time neural network control of a robotic manipulator with input deadzone,” *ISA Transactions*, vol. 135, pp. 449–461, 2023. [Online]. Available: <https://www.sciencedirect.com/science/article/pii/S0019057822004876>
- [6] P. Schuchert and A. Karimi, “Data-driven frequency-based feedforward control design for a robotic arm joint,” in *2024 American Control Conference (ACC)*, 2024, pp. 3853–3858.
- [7] B. K. Oleiwi, M. Jasim, A. T. Azar, S. Ahmed, and A. R. Mahlous, “Bat optimization of hybrid neural network-fopid controllers for robust robot manipulator control,” *Frontiers in Robotics and AI*, vol. Volume 12 - 2025, 2025. [Online]. Available: <https://www.frontiersin.org/journals/robotics-and-ai/articles/10.3389/frobt.2025.1487844>

- [8] S. Schneider and F. Kummert, "Comparing robot and human guided personalization: Adaptive exercise robots are perceived as more competent and trustworthy," *International journal of social robotics*, vol. 13, no. 2, pp. 169–185, Apr. 2021.
- [9] A. Tanevska, F. Rea, G. Sandini, L. Cañamero, and A. Sciutti, "A Socially Adaptable Framework for Human-Robot Interaction," *Frontiers in Robotics and AI*, vol. 7, p. 121, 2020. [Online]. Available: <https://doi.org/10.3389/frobt.2020.00121>
- [10] S. Nikolaidis, D. Hsu, and S. S. Srinivasa, "Human-robot mutual adaptation in collaborative tasks: Models and experiments," *The International Journal of Robotics Research*, vol. 36, no. 5-7, pp. 618–634, 2017. [Online]. Available: <https://doi.org/10.1177/0278364917690593>
- [11] L. Treven, B. Sukhija, Y. As, F. Dörfler, and A. Krause, "When to sense and control? a time-adaptive approach for continuous-time rl," in *Advances in Neural Information Processing Systems*, A. Globerson, L. Mackey, D. Belgrave, A. Fan, U. Paquet, J. Tomczak, and C. Zhang, Eds., vol. 37. Curran Associates, Inc., 2024, pp. 63 654–63 685. [Online]. Available: https://proceedings.neurips.cc/paper_files/paper/2024/file/746b0a1e6e3cfff8d968ba6d2e6fff049-Paper-Conference.pdf
- [12] S. Park, J. Kim, and G. Kim, "Time discretization-invariant safe action repetition for policy gradient methods," in *Advances in Neural Information Processing Systems*, M. Ranzato, A. Beygelzimer, Y. Dauphin, P. Liang, and J. W. Vaughan, Eds., vol. 34. Curran Associates, Inc., 2021, pp. 267–279. [Online]. Available: https://proceedings.neurips.cc/paper_files/paper/2021/file/024677efb8e4ae2eaeef17b54695bbe-Paper.pdf
- [13] S. Amin, M. Gomrokchi, H. Aboutaleb, H. Satija, and D. Precup, "Locally persistent exploration in continuous control tasks with sparse rewards," in *Proceedings of the 38th International Conference on Machine Learning*, ser. Proceedings of Machine Learning Research, M. Meila and T. Zhang, Eds., vol. 139. PMLR, 18–24 Jul 2021, pp. 275–285. [Online]. Available: <https://proceedings.mlr.press/v139/amin21a.html>
- [14] A. Karimi, J. Jin, J. Luo, A. R. Mahmood, M. Jagersand, and S. Tosatto, "Dynamic decision frequency with continuous options," in *2023 IEEE/RSJ International Conference on Intelligent Robots and Systems (IROS)*, 2023, pp. 7545–7552.
- [15] D. Wang and G. Beltrame, "Moseac: Streamlined variable time step reinforcement learning," 2024. [Online]. Available: <https://arxiv.org/abs/2406.01521>
- [16] S. Gangapurwala, L. Campanaro, and I. Havoutis, "Learning low-frequency motion control for robust and dynamic robot locomotion," in *2023 IEEE International Conference on Robotics and Automation (ICRA)*, 2023, pp. 5085–5091.
- [17] C. Nguyen, A. Altawaitan, T. Duong, N. Atanasov, and Q. Nguyen, "Variable-frequency model learning and predictive control for jumping maneuvers on legged robots," *IEEE Robotics and Automation Letters*, vol. 10, no. 2, pp. 1321–1328, 2025.
- [18] Y. Li, Y. Zhang, W. Xiao, C. Pan, H. Weng, G. He, T. He, and G. Shi, "Hold my beer: Learning gentle humanoid locomotion and end-effector stabilization control," in *RSS 2025 Workshop on Whole-body Control and Bimanual Manipulation: Applications in Humanoids and Beyond*, 2025. [Online]. Available: <https://openreview.net/forum?id=2ajP0TMxi7>
- [19] D. Hafner, T. Lillicrap, J. Ba, and M. Norouzi, "Dream to control: Learning behaviors by latent imagination," in *International Conference on Learning Representations*, 2020. [Online]. Available: <https://openreview.net/forum?id=S11OTC4tDS>
- [20] A. Braylan, M. Hollenbeck, E. Meyerson, and R. Miikkulainen, "Frame skip is a powerful parameter for learning to play atari," in *AAAI-15 Workshop on Learning for General Competency in Video Games*, 2015. [Online]. Available: <http://nn.cs.utexas.edu/?braylan:aaai15ws>
- [21] S. Sharma, A. S. Lakshminarayanan, and B. Ravindran, "Learning to repeat: Fine grained action repetition for deep reinforcement learning," in *International Conference on Learning Representations*, 2017.
- [22] A. M. Metelli, F. Mazzolini, L. Bisi, L. Sabbioni, and M. Restelli, "Control frequency adaptation via action persistence in batch reinforcement learning," in *Proceedings of the 37th International Conference on Machine Learning*, ser. Proceedings of Machine Learning Research, H. D. III and A. Singh, Eds., vol. 119. PMLR, 13–18 Jul 2020, pp. 6862–6873. [Online]. Available: <https://proceedings.mlr.press/v119/metelli20a.html>
- [23] D. Wang and G. Beltrame, "Reinforcement learning with elastic time steps," 2024. [Online]. Available: <https://arxiv.org/abs/2402.14961>
- [24] T. Haarnoja, A. Zhou, P. Abbeel, and S. Levine, "Soft actor-critic: Off-policy maximum entropy deep reinforcement learning with a stochastic actor," in *International conference on machine learning*. Pmlr, 2018, pp. 1861–1870.
- [25] J. Li, Z. Duan, J. Ma, and Q. Nguyen, "Gait-net-augmented implicit kino-dynamic mpc for dynamic variable-frequency humanoid locomotion over discrete terrains," 2025. [Online]. Available: <https://arxiv.org/abs/2502.02934>
- [26] W. Heemels, K. Johansson, and P. Tabuada, "An introduction to event-triggered and self-triggered control," in *2012 IEEE 51st IEEE Conference on Decision and Control (CDC)*, 2012, pp. 3270–3285.
- [27] A. Anta and P. Tabuada, "To sample or not to sample: Self-triggered control for nonlinear systems," *IEEE Transactions on Automatic Control*, vol. 55, no. 9, pp. 2030–2042, 2010.
- [28] J. Schulman, F. Wolski, P. Dhariwal, A. Radford, and O. Klimov, "Proximal policy optimization algorithms," 2017. [Online]. Available: <https://arxiv.org/abs/1707.06347>
- [29] C. D. Freeman, E. Frey, A. Raichuk, S. Girgin, I. Mordatch, and O. Bachem, "Brax - a differentiable physics engine for large scale rigid body simulation," in *Thirty-fifth Conference on Neural Information Processing Systems Datasets and Benchmarks Track (Round 1)*, 2021. [Online]. Available: <https://openreview.net/forum?id=VdvDlnnJzIN>
- [30] A. Bhardwaj, J. Rothfuss, B. Sukhija, Y. As, M. Hutter, S. Coros, and A. Krause, "Data-efficient task generalization via probabilistic model-based meta reinforcement learning," *IEEE Robotics and Automation Letters*, vol. 9, no. 4, pp. 3918–3925, 2024.
- [31] B. Sukhija, N. Köhler, M. Zamora, S. Zimmermann, S. Curi, A. Krause, and S. Coros, "Gradient-based trajectory optimization with learned dynamics," in *2023 IEEE International Conference on Robotics and Automation (ICRA)*, 2023, pp. 1011–1018.
- [32] OptiTrack, "Robotics Motion Capture Systems," <https://optitrack.com/applications/robotics/>, 2024, accessed: July 22, 2024.
- [33] J. Kabzan, M. I. Valls, V. J. F. Reijgwart, H. F. C. Hendrikx, C. Ehmke, M. Prajapat, A. Bühler, N. Gosala, M. Gupta, R. Sivanesan, A. Dhall, E. Chisari, N. Karnchanachari, S. Brits, M. Dangel, I. Sa, R. Dubé, A. Gawel, M. Pfeiffer, A. Liniger, J. Lygeros, and R. Siegwart, "Amz driverless: The full autonomous racing system," *Journal of Field Robotics*, vol. 37, no. 7, pp. 1267–1294, 2020. [Online]. Available: <https://onlinelibrary.wiley.com/doi/abs/10.1002/rob.21977>
- [34] H. B. Pacejka and E. Bakker, "The magic formula tyre model," *Vehicle System Dynamics*, vol. 21, no. sup001, pp. 1–18, 1992. [Online]. Available: <https://doi.org/10.1080/00423119208969994>
- [35] J. Tobin, R. Fong, A. Ray, J. Schneider, W. Zaremba, and P. Abbeel, "Domain randomization for transferring deep neural networks from simulation to the real world," in *2017 IEEE/RSJ International Conference on Intelligent Robots and Systems (IROS)*, 2017, pp. 23–30.
- [36] J. Rothfuss, B. Sukhija, L. Treven, F. Dörfler, S. Coros, and A. Krause, "Bridging the sim-to-real gap with bayesian inference," in *2024 IEEE/RSJ International Conference on Intelligent Robots and Systems (IROS)*, 2024, pp. 10 784–10 791.
- [37] Y. Tassa, Y. Doron, A. Muldal, T. Erez, Y. Li, D. de Las Casas, D. Budden, A. Abdolmaleki, J. Merel, A. Lefrancq, T. Lillicrap, and M. Riedmiller, "Deepmind control suite," 2018. [Online]. Available: <https://arxiv.org/abs/1801.00690>
- [38] Unitree Robotics, "Go1 Quadruped Robot," <https://www.unitree.com/go1>, 2024, accessed: July 22, 2024.
- [39] K. Zakka, B. Tabanpour, Q. Liao, M. Haiderbhai, S. Holt, J. Y. Luo, A. Allshire, E. Frey, K. Sreenath, L. A. Kahrs, C. Sferrazza, Y. Tassa, and P. Abbeel, "Mujoco playground," 2025. [Online]. Available: <https://arxiv.org/abs/2502.08844>
- [40] ONNX Community, "ONNX: Open Neural Network Exchange," <https://onnx.ai/>, 2024, accessed: July 22, 2024.
- [41] G. Ji, J. Mun, H. Kim, and J. Hwangbo, "Concurrent training of a control policy and a state estimator for dynamic and robust legged locomotion," *IEEE Robotics and Automation Letters*, vol. 7, no. 2, p. 4630–4637, Apr. 2022. [Online]. Available: <http://dx.doi.org/10.1109/LRA.2022.3151396>
- [42] N. Rudin, D. Hoeller, P. Reist, and M. Hutter, "Learning to walk in minutes using massively parallel deep reinforcement learning," in *Proceedings of the 5th Conference on Robot Learning*, ser. Proceedings of Machine Learning Research, A. Faust, D. Hsu, and G. Neumann, Eds., vol. 164. PMLR, 08–11 Nov 2022, pp. 91–100. [Online]. Available: <https://proceedings.mlr.press/v164/rudin22a.html>

- [43] C. D. Bellicoso, F. Jenelten, C. Gehring, and M. Hutter, "Dynamic locomotion through online nonlinear motion optimization for quadrupedal robots," *IEEE Robotics and Automation Letters*, vol. 3, no. 3, pp. 2261–2268, 2018.
- [44] L. Pinto, M. Andrychowicz, P. Welinder, W. Zaremba, and P. Abbeel, "Asymmetric actor critic for image-based robot learning;" 2017. [Online]. Available: <https://arxiv.org/abs/1710.06542>